Supporting Information

Effective Anisotropic Interactions in Spin-Pairs Containing High Spin Ions with Large Zero-Field Splitting

Nicolás I. Neuman,*

Departamento de Física, FBCB-UNL, CONICET, Facultad de Bioquímica y Ciencias Biológicas, Ciudad Universitaria, Ruta N 168 S/N, S3000ZAA Santa Fe, Argentina

8.References

1. Introduction

The magnetic properties of high spin Co(II) ions (S = 3/2) have been thoroughly studied by experimental and theoretical methods.[1-7] The S = 3/2 spin experiences a *zero-field splitting* (ZFS) which splits the spin multiplet into two doublets which, in the main direction of the ZFS **D**-tensor, can be labeled as $M_S = \pm 1/2$ and $M_S = \pm 3/2$. The real spin S = 3/2 has, apart from the **D**-tensor which causes the ZFS, a "real" **g**-matrix which is anisotropic with values around the 2-3 range. The origin of these interactions is the admixture caused by the spin-orbit coupling of the orbital magnetic moment of the ground and excited states into the spin magnetic properties. This admixture is dependent on the energy separations between the different orbital sub-levels arising from the parent ^4F and ^4P terms under the octahedral, tetragonal and lower crystal field distortions. These properties can be analyzed at several different levels of theory[1] including multiconfigurational electronic structure calculations.[8, 9] In EPR spectroscopic studies at X-band it is not necessary, although not unadvisable, to be concerned with the orbital origin of the magnetic properties, as only the pure spin Hamiltonian is strictly needed to analyze the results. Furthermore, as the ZFS is usually much larger than the microwave energy at X-, Q- and even W-band, only transitions between the lower doublet are observed, to which an effective S´ = 1/2 spin can be assigned and which present resonance positions given by an effective **g**´-matrix.

ZFS of some kind is experienced by other high spin ions such as Fe(III) (S = 5/2), Mn(II) (S = 5/2) and some lanthanides, with the magnetic properties depending on the magnitude of the ZFS and the orbital contributions to the **g**-matrix. In this work we center the analysis on spin pairs containing Co(II) or Fe(III) ions which can be treated in certain experiments as effective S´=1/2 systems.

2. Pilbrow's equations for S = 3/2

The relations between the effective **g**´-matrix components, the real **g**-matrix and the λ = E/D rhombicity parameter of the *zero-field splitting* have been given by Pilbrow.[2] These expressions are written below for S = 3/2

$$\left.\begin{aligned} g'_x &= g_x\left(1 \pm \frac{1-3\lambda}{\sqrt{1+3\lambda^2}}\right) \\ g'_y &= g_y\left(1 \pm \frac{1+3\lambda}{\sqrt{1+3\lambda^2}}\right) \\ g'_z &= g_z\left(1 \mp \frac{2}{\sqrt{1+3\lambda^2}}\right) \end{aligned}\right\} + O\left(\left(\frac{g_i \mu_B B}{D\sqrt{1+3\lambda^2}}\right)^2\right) \qquad (1)$$

The upper signs refer to the $M_S = \pm 1/2$ and the lower signs to the $M_S = \pm 3/2$ doublets. Terms containing $\left(g_i \mu_B B/D\right)^2$ are disregarded because they are too small in most cases, but can be obtained from Pilbrow's work.

3. Derivation of formulae for the effective *g´* values for S = 5/2.

For S ≥ 3/2 in axial symmetry (E = 0) some formulas reviewed by Pilbrow[2] are

$$g' = g_e\left(1 - \frac{(S+3/2)(S-1/2)}{(2S+1)^2}\left(\frac{g_\perp \mu_B B}{2D}\right)^2 \sin^2\theta\left[1 - 3\left(\frac{g_\parallel}{g_e}\right)^2 \cos^2\theta\right]\right)$$

Where

$$g_e^2 = g_{\parallel}^2 \cos^2\theta + g_{\perp}^2 (S+1/2)^2 \sin^2\theta$$

For S = 5/2, one then obtains for the $M_S = \pm 1/2$ doublet

$$g' = g_e \left(1 - \frac{1}{18} \left(\frac{g_{\perp} \mu_B B}{D} \right)^2 \sin^2\theta \left[1 - 3 \left(\frac{g_{\parallel}}{g_e} \right)^2 \cos^2\theta \right] \right)$$

So in the *xy* plane, where θ = 90º, $g'_{\perp} = g' = 3g_{\perp}\left(1 - (g_{\perp}\mu_B B/D)^2/18\right)$ and in the *z* direction, where θ = 0º, $g'_z = g_{\parallel}$.

To the best of the authors' knowledge no analytical expressions have been derived for effective **g**′-matrix components of an S = 5/2 or larger system when rhombic ZFS is present. We attempted to derive analytical formulae for the effective *g*′-values of an S = 5/2 system using a mixture of exact diagonalization of the 6 × 6 matrices arising from the Hamiltonian (eq. 2)

$$\hat{H}_{5/2} = D\left(\hat{S}_z^2 - 35/12\right) + E\left(\hat{S}_x^2 - \hat{S}_y^2\right) \qquad (2)$$

plus introduction of the Zeeman interaction in a perturbative fashion, and obtained approximate formulae which to our opinion were not similar enough to the exact numerically calculated *g*′-values; we also realized that more exact expressions would be too complicated to be of any practical use. Therefore, in the need to calculate effective *g*′-values as a function of the E/D parameter, we simply fit the exact numerical calculations with second order polynomials (eq. 3).

$$g'_u = a_0 + a_1(E/D) + a_2(E/D)^2 \qquad (3)$$

The fittings are shown in Figure S1 and the polynomial coefficients are given in Table S1. These coefficients assume a real isotropic *g*-value of 2, which is a common approximation for Fe(III) ions. If a different real *g*-value need be considered, each expression can be multiplied by the factor (*g*/2).

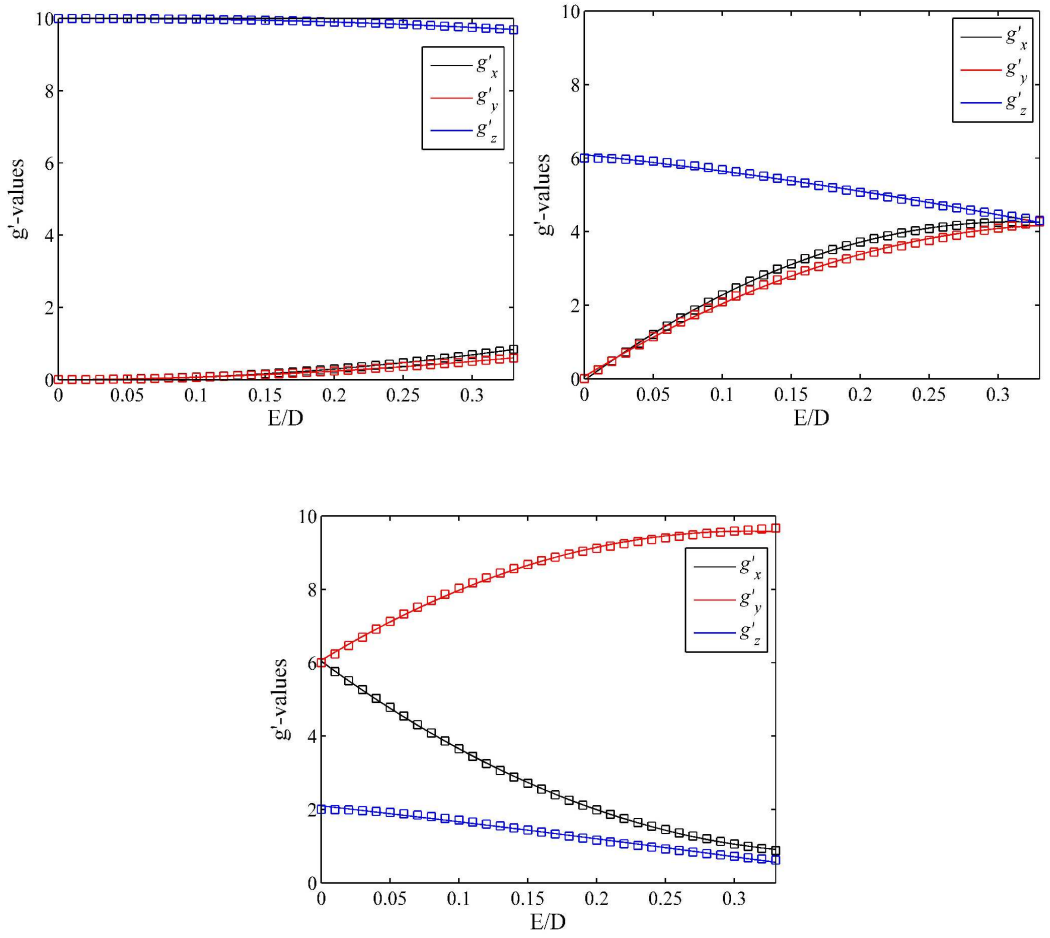

Figure S1. Numerical (symbols) and analytic approximate (lines) effective *g′*-values for the $M_S = \pm 5/2$ (top), $M_S = \pm 3/2$ (center) and $M_S = \pm 1/2$ (bottom) Kramer's doublets of an S = 5/2 spin with axial and rhombic ZFS, as a function of E/D. The *xyz* axes follow the common convention for rhombic ZFS, as shown in eq. 2.

Table S1. Coefficients of polynomial expression (eq. 3) fitting each Kramer's doublet in an S = 5/2 spin with rhombic ZFS.

$M_S = \pm 1/2$	a_0	a_1	a_2	$M_S = \pm 3/2$	a_0	a_1	a_2	$M_S = \pm 5/2$	a_0	a_1	a_2
g'_x	6.0	-26.96	34.87	g'_x	0.0	27.09	-42.94	g'_x	0.0	-0.13	8.06
g'_y	6.0	23.57	-38.81	g'_y	0.0	23.68	-33.62	g'_y	0.0	0.17	5.05
g'_z	2.0	-3.04	-4.32	g'_z	6.0	-2.91	-7.51	g'_z	10.0	0.13	-3.19

4. Effective interactions for two interacting S = 3/2 ions

Recently we have developed formulae for the effective anisotropic exchange interaction between two S = 3/2 Co(II) ions which are valid when a real isotropic interaction J couples two equivalent ions and the ZFS is much larger than J.[10]

For two equivalent S = 3/2 ions coupled by an isotropic exchange interaction $J^{3/2}$, each experiencing a ZFS with a positive D value defining the z direction, the EPR signals at low temperature and microwave frequency much lower than D, can be analyzed as the result of two interacting S′ = 1/2 spins with an effective anisotropic exchange interaction $\mathbf{J}^{1/2}_{\text{ani}}$, whose components are given below (eq. 4), with the effective isotropic exchange interaction $J^{1/2}$ already subtracted.

$$\begin{aligned} J^{1/2} &= 3J^{3/2} \\ J^{1/2}_{\text{ani,z}} &= -2J^{3/2} \\ J^{1/2}_{\text{ani,y}} &= J^{1/2}_{\text{ani,x}} = J^{3/2} \end{aligned} \qquad (4)$$

If the real S = 3/2 spins also experience anisotropic interactions such as anisotropic exchange ($\mathbf{J}^{3/2}$) or dipolar interaction ($\mathbf{D}^{3/2}_{\text{dip}}$), these interactions will also give rise to effective anisotropic interactions if the spins are analyzed as S′ = 1/2.

Initially our extension of the effective interaction formulas for arbitrary interactions (real and effective) was performed for certain symmetrical situations in which the interspin (anisotropic exchange or dipolar) interaction shared axes with both ions ZFS tensors. After obtaining these relations (eqs. (12), (13) and (14) shown below), their mathematical expressions made us realize that the formulas for effective magnetic interactions could be expressed generally for any pair of effective spins, regardless of the relative orientations of each ions ZFS and the interspin interaction. For purposes of showing our reasoning to the reader we will present the deduction of formulas for high symmetry situations, and then prove their general validity through the simulation of particular cases: a pair of high-spin Co(II) ions (Figure 1 in the main text) and a high-spin Fe(III)-Cu(II) spin pair (Figure S4 in this Supplementary Material).

Our previous work was based on Pilbrow's work[2] on effective **g**′-matrices for high-spin Co(II) ions. The eigenvalues and eigenvectors of the Hamiltonian

$$\mathrm{H}_{\mathrm{ZFS}}=D_k\left(S_{k,z}^2-5/4\right)+\frac{E}{2}\left(S_{k,+}^2+S_{k,-}^2\right) \tag{5}$$

for an S = 3/2 spin, where *k* indicates a given Co(II) ion, are

$$\begin{aligned}\varepsilon_{1,2}^k&=D_k\sqrt{\left(1+\lambda_k^2\right)}\\ \varepsilon_{3,4}^k&=-D_k\sqrt{\left(1+\lambda_k^2\right)}\\ \lambda_k&=\frac{E_k}{D_k}\end{aligned} \tag{6}$$

and

$$
\begin{aligned}
|\varphi_{k1}\rangle &= a_k \left|(3/2)_k\right\rangle + b_k \left|(-1/2)_k\right\rangle \\
|\varphi_{k2}\rangle &= c_k \left|(1/2)_k\right\rangle + d_k \left|(-3/2)_k\right\rangle \\
|\varphi_{k3}\rangle &= -c_k \left|(3/2)_k\right\rangle + d_k \left|(-1/2)_k\right\rangle \\
|\varphi_{k4}\rangle &= -a_k \left|(1/2)_k\right\rangle + b_k \left|(-3/2)_k\right\rangle
\end{aligned}
\tag{7}
$$

where

$$
\begin{aligned}
a_k &= \frac{\left(3\lambda_k^2+1\right)^{1/2}+1}{\sqrt{2}\left\{\left(3\lambda_k^2+1\right)+\left(3\lambda_k^2+1\right)^{1/2}\right\}^{1/2}} \\
b_k &= \frac{\sqrt{3}\lambda_k}{\sqrt{2}\left\{3\lambda_k^2+1+\left(3\lambda_k^2+1\right)^{1/2}\right\}} \\
c_k &= \frac{\left(3\lambda_k^2+1\right)^{1/2}-1}{\sqrt{2}\left\{\left(3\lambda_k^2+1\right)-\left(3\lambda_k^2+1\right)^{1/2}\right\}^{1/2}} \\
d_k &= \frac{\sqrt{3}\lambda_k}{\sqrt{2}\left\{3\lambda_k^2+1-\left(3\lambda_k^2+1\right)^{1/2}\right\}^{1/2}}
\end{aligned}
\tag{8}
$$

The four eigenvectors can be grouped in two Kramers' doublets, as shown in Figure S2.

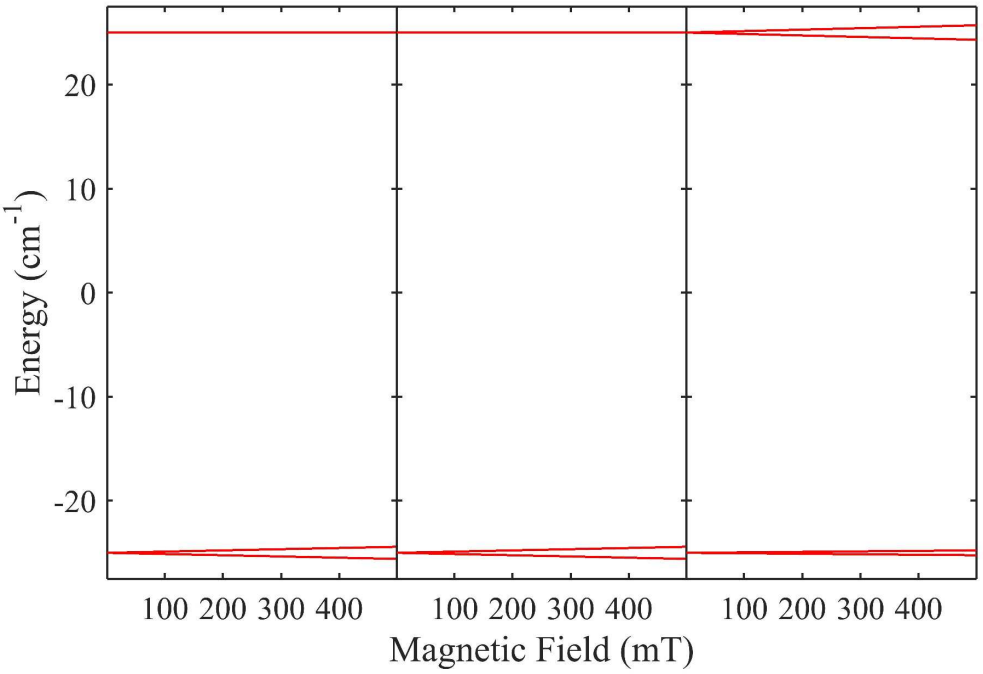

Figure S2. Energy levels for a high-spin Co(II) ion with positive ZFS (D = 25 cm^{-1}, E/D = 0.05) with external magnetic field pointing in the *x* (left), *y* (center) and *z* (right) directions, given by the principal axes system of the **D**-tensor. Real *g*-values in the *x*, *y*, *z* order are 2.5, 2.5, 2.0.

Orthonormality of the eigenvectors of a Hamiltonian imply that $a_k = d_k$ and $b_k = c_k$ (although it would not be easily seen by inspection of the formulas). Therefore the lower Kramer's doublets are φ_{k3} and φ_{k4}, and given by

$$\begin{aligned} \left|\varphi_{k3}\right\rangle &= -b_k\left|+3/2\right\rangle + a_k\left|-1/2\right\rangle = \begin{bmatrix} -b_k & 0 & a_k & 0 \end{bmatrix} \cdot \begin{bmatrix} +3/2 \\ +1/2 \\ -1/2 \\ -3/2 \end{bmatrix} \\ \left|\varphi_{k4}\right\rangle &= -a_k\left|+1/2\right\rangle + b_k\left|-3/2\right\rangle = \begin{bmatrix} 0 & -a_k & 0 & b_k \end{bmatrix} \cdot \begin{bmatrix} +3/2 \\ +1/2 \\ -1/2 \\ -3/2 \end{bmatrix} \end{aligned} \tag{9}$$

If a pair of high spin Co(II) ions interact with an interaction much smaller than each ion's ZFS, the Hamiltonian

$$H_{AB}^{HS} = \hat{\mathbf{S}}_A \cdot \mathbf{J}^{HS} \cdot \hat{\mathbf{S}}_B \tag{10}$$

can be truncated in order to include only each ion's lower eigenstates (i.e. lower Kramers' doublets). Application of Hamiltonian (eq. 10) to the direct product $[\varphi_{A3}\ \varphi_{A4}]\otimes[\varphi_{B3}\ \varphi_{B4}]$ would give a 16 × 16 energy matrix. The way in which matrix is formed is given in eq. 11

$$\mathbf{H}_{AB}^{eff} = \begin{bmatrix} \langle\varphi_{A3}\varphi_{B3}| \\ \langle\varphi_{A3}\varphi_{B4}| \\ \langle\varphi_{A4}\varphi_{B3}| \\ \langle\varphi_{A4}\varphi_{B4}| \end{bmatrix} \left(\hat{\mathbf{S}}_A \cdot \mathbf{J}^{HS} \cdot \hat{\mathbf{S}}_B\right) \left[|\varphi_{A3}\varphi_{B3}\rangle\ |\varphi_{A3}\varphi_{B4}\rangle\ |\varphi_{A4}\varphi_{B3}\rangle\ |\varphi_{A4}\varphi_{B4}\rangle\right] \tag{11}$$

Substitution of expression (eq. 9) into the matrix (eq. 11), carrying on all the calculations of matrix elements of the type $\langle M_{SA}M_{SB}|\hat{S}_{Au}\hat{S}_{Bv}|M'_{SA}M'_{SB}\rangle$ with $u,v = x, y, z$, gives, as said before, a 16 × 16 energy matrix. However, as couplings with eigenstates containing φ_{k1} and φ_{k2}, have been disregarded due to the large $ZFS_A/\mathbf{J}_{AB}$ and $ZFS_B/\mathbf{J}_{AB}$ ratios, this matrix can be block diagonalized into two 4 × 4 matrices.

Let us assume that the anisotropic interaction between the real S = 3/2 spins ($\mathbf{D}^{3/2}$) has components $D_x^{3/2}$, $D_y^{3/2}$ and $D_z^{3/2}$, without any assumption as to the relative values of the different components, except for a null trace. Then, the formulae obtained in our previous work[10] can be extended as

$$H_{ex}^{1/2}=\begin{pmatrix} D_z^{3/2}\dfrac{\left(a_A^2-3b_A^2\right)\left(a_B^2-3b_B^2\right)}{4} & 0 & 0 & D_x^{3/2}\left(a_Aa_B\right)\begin{pmatrix} a_Aa_B+3b_Ab_B \\ -\sqrt{3}\left(a_Ab_B+b_Aa_B\right)\end{pmatrix}- \\ & & & D_y^{3/2}\left(a_Aa_B\right)\begin{pmatrix} a_Aa_B+3b_Ab_B \\ +\sqrt{3}\left(a_Ab_B+b_Aa_B\right)\end{pmatrix} \\ 0 & -D_z^{3/2}\dfrac{\left(a_A^2-3b_A^2\right)\left(a_B^2-3b_B^2\right)}{4} & D_x^{3/2}\left(a_Aa_B\right)\begin{pmatrix} a_Aa_B+3b_Ab_B \\ -\sqrt{3}\left(a_Ab_B+b_Aa_B\right)\end{pmatrix}+ & 0 \\ & & D_y^{3/2}\left(a_Aa_B\right)\begin{pmatrix} a_Aa_B+3b_Ab_B \\ +\sqrt{3}\left(a_Ab_B+b_Aa_B\right)\end{pmatrix} & \\ 0 & D_x^{3/2}\left(a_Aa_B\right)\begin{pmatrix} a_Aa_B+3b_Ab_B \\ -\sqrt{3}\left(a_Ab_B+b_Aa_B\right)\end{pmatrix}+ & -D_z^{3/2}\dfrac{\left(a_A^2-3b_A^2\right)\left(a_B^2-3b_B^2\right)}{4} & 0 \\ & D_y^{3/2}\left(a_Aa_B\right)\begin{pmatrix} a_Aa_B+3b_Ab_B \\ +\sqrt{3}\left(a_Ab_B+b_Aa_B\right)\end{pmatrix} & & \\ D_x^{3/2}\left(a_Aa_B\right)\begin{pmatrix} a_Aa_B+3b_Ab_B \\ -\sqrt{3}\left(a_Ab_B+b_Aa_B\right)\end{pmatrix}- & 0 & 0 & D_z^{3/2}\dfrac{\left(a_A^2-3b_A^2\right)\left(a_B^2-3b_B^2\right)}{4} \\ D_y^{3/2}\left(a_Aa_B\right)\begin{pmatrix} a_Aa_B+3b_Ab_B \\ +\sqrt{3}\left(a_Ab_B+b_Aa_B\right)\end{pmatrix} & & & \end{pmatrix}$$

This energy matrix has the same shape as the energy matrix of two effective $S' = 1/2$ spins interacting by a diagonal tensor $\mathbf{J}^{\text{eff}}$, as will be shown further below.

The following step is to assume that the A and B sites are equivalent (which is not a problem because previously it was assumed that they had the same ZFS directions)

$$H_{ex}^{1/2}=\begin{pmatrix} D_z^{3/2}\dfrac{\left(a^2-3b^2\right)\left(a^2-3b^2\right)}{4} & 0 & 0 & D_x^{3/2}\left(a^2\right)\begin{pmatrix}a^2+3b^2\\-2\sqrt{3}ab\end{pmatrix}- D_y^{3/2}\left(a^2\right)\begin{pmatrix}a^2+3b^2\\+2\sqrt{3}ab\end{pmatrix} \\ 0 & -D_z^{3/2}\dfrac{\left(a^2-3b^2\right)\left(a^2-3b^2\right)}{4} & D_x^{3/2}\left(a^2\right)\begin{pmatrix}a^2+3b^2\\-2\sqrt{3}ab\end{pmatrix}+ D_y^{3/2}\left(a^2\right)\begin{pmatrix}a^2+3b^2\\+2\sqrt{3}ab\end{pmatrix} & 0 \\ 0 & D_x^{3/2}\left(a^2\right)\begin{pmatrix}a^2+3b^2\\-2\sqrt{3}ab\end{pmatrix}+ D_y^{3/2}\left(a^2\right)\begin{pmatrix}a^2+3b^2\\+2\sqrt{3}ab\end{pmatrix} & -D_z^{3/2}\dfrac{\left(a^2-3b^2\right)\left(a^2-3b^2\right)}{4} & 0 \\ D_x^{3/2}\left(a^2\right)\begin{pmatrix}a^2+3b^2\\-2\sqrt{3}ab\end{pmatrix}- D_y^{3/2}\left(a^2\right)\begin{pmatrix}a^2+3b^2\\+2\sqrt{3}ab\end{pmatrix} & 0 & 0 & D_z^{3/2}\dfrac{\left(a^2-3b^2\right)\left(a^2-3b^2\right)}{4} \end{pmatrix}$$

Now if we further assume that the rhombicity is nearly 0 (a= 1, b = 0), we get a much simplified expression.

$$H_{ex}^{1/2}=\begin{pmatrix} \dfrac{D_z^{3/2}}{4} & 0 & 0 & D_x^{3/2}-D_y^{3/2} \\ 0 & -\dfrac{D_z^{3/2}}{4} & D_x^{3/2}+D_y^{3/2} & 0 \\ 0 & D_x^{3/2}+D_y^{3/2} & -\dfrac{D_z^{3/2}}{4} & 0 \\ D_x^{3/2}-D_y^{3/2} & 0 & 0 & \dfrac{D_z^{3/2}}{4} \end{pmatrix}$$

By comparing this energy matrix with the one arising from the effective spin exchange Hamiltonian $H_{exch}^{eff}=+\mathbf{S'}_A\cdot\mathbf{D}_{AB}^{1/2}\cdot\mathbf{S'}_B$ in the $\mathbf{S'}_A=\mathbf{S'}_B=1/2$ effective basis

$$\begin{pmatrix} \frac{D_z^{1/2}}{4} & 0 & 0 & \frac{D_x^{1/2}-D_y^{1/2}}{4} \\ 0 & -\frac{D_z^{1/2}}{4} & \frac{D_x^{1/2}+D_y^{1/2}}{4} & 0 \\ 0 & \frac{D_x^{1/2}+D_y^{1/2}}{4} & -\frac{D_z^{1/2}}{4} & 0 \\ \frac{D_x^{1/2}-D_y^{1/2}}{4} & 0 & 0 & \frac{D_z^{1/2}}{4} \end{pmatrix}$$

We get

$$\begin{aligned} D_z^{1/2} &= D_z^{3/2} \\ D_x^{1/2} + D_y^{1/2} &= 4\left(D_x^{3/2} + D_y^{3/2}\right) \\ D_x^{1/2} - D_y^{1/2} &= 4\left(D_x^{3/2} - D_y^{3/2}\right) \end{aligned}$$

Which coincides with the expressions in eq. 12 when E/D = 0.

$$\begin{aligned} D_x^{1/2} &= 4D_x^{3/2} = D_x^{3/2}\left(1+\frac{1-3\left(E/D\right)}{\sqrt{1+3\left(E/D\right)^2}}\right)^2 \\ D_y^{1/2} &= 4D_y^{3/2} = D_y^{3/2}\left(1+\frac{1+3\left(E/D\right)}{\sqrt{1+3\left(E/D\right)^2}}\right)^2 \\ D_z^{1/2} &= D_z^{3/2} = D_z^{3/2}\left(1-\frac{2}{\sqrt{1+3\left(E/D\right)^2}}\right)^2 \end{aligned} \qquad (12)$$

In this case we also consider that the real $\mathbf{D}^{3/2}$ tensor has zero-trace, because all the isotropic part would have gone into the $J^{3/2} \rightarrow J^{1/2}+\mathbf{J}^{1/2}_{\text{ani}}$ relations. In the case of high rhombicity (E/D = 1/3), $b_1 = 0.9659$ and $b_2 = 0.2588$), we have

$$H_{ex}^{1/2} = \begin{pmatrix} 0.5359\dfrac{D_z^{3/2}}{4} & 0 & 0 & 0.25D_x^{3/2} - 1.866D_y^{3/2} \\ 0 & -0.5359\dfrac{D_z^{3/2}}{4} & 0.25D_x^{3/2} + 1.866D_y^{3/2} & 0 \\ 0 & 0.25D_x^{3/2} + 1.866D_y^{3/2} & -0.5359\dfrac{D_z^{3/2}}{4} & 0 \\ 0.25D_x^{3/2} - 1.866D_y^{3/2} & 0 & 0 & 0.5359\dfrac{D_z^{3/2}}{4} \end{pmatrix}$$

Following the same procedure than for the E/D = 0 case, we find the following relations.

$$\begin{aligned} D_x^{1/2} &= D_x^{3/2} = D_x^{3/2}\left(1+\frac{1-3(E/D)}{\sqrt{1+3(E/D)^2}}\right)^2 \\ D_y^{1/2} &= 7.464D_y^{3/2} = D_y^{3/2}\left(1+\frac{1+3(E/D)}{\sqrt{1+3(E/D)^2}}\right)^2 \\ D_z^{1/2} &= 0.5359D_z^{3/2} = D_z^{3/2}\left(1-\frac{2}{\sqrt{1+3(E/D)^2}}\right)^2 \end{aligned} \qquad (13)$$

It has to be noted that in the way that E/D is defined as positive, $D^{ZFS}{}_x > D^{ZFS}{}_y$, so clear knowledge of the values of the *x* and *y* components of both the zero-field splitting and the Co(II)-Co(II) real anisotropic interaction is necessary to use the previous formulae.

We have to confess that observation that the coefficients multiplying the real *D*-components are indeed the Pilbrow factors for the *g*-values squared was made *a posteriori* by observation of the numerical results. Initially we thought that the relations obtained in our previous work[10] were only useful for a real isotropic exchange $J^{3/2}$, and that we would only be able to derive similar formulas for anisotropic interactions in certain high symmetry situations. The simplicity of the obtained results made sense *a posteriori*, and this insight allowed us to propose more general equations for the effective interactions. This relations

are proved in this work by simulation of the energy levels of an interaction system of S = 3/2 or S = 5/2 ions in both the real spin formulation and the effective spin formulation.

Equations 12 and 13 show, for example, that if two Co(II) ions have ZFS principal directions perpendicular to the Co(II)-Co(II) vector, depending on the relative orientation of the ZFS *x* and *y* eigenvectors, the effective anisotropic interaction can be much larger than the real anisotropic interaction.

Now we will explore a few situations in which the Co(II) pair has different relative orientations and rhombicities (Figure S3)

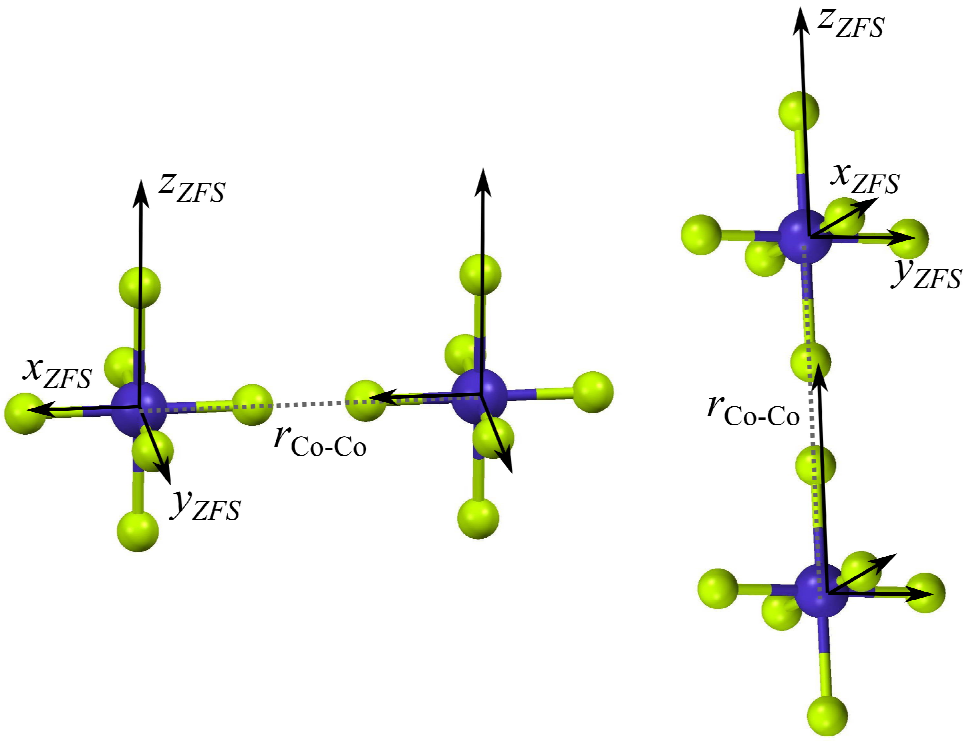

Figure S3. Relative orientations of the Co-Co vector and the ZFS principal axis. (Left) perpendicular directions, (right) colinear directions.

The general expression for the real dipolar interaction tensor is

$$D_{dip}^{3/2} = \mu_B^2 \hbar^2 \frac{\mu_0}{4\pi r^3} \left(\mathbf{g}_1^T \cdot \mathbf{g}_2 - 3 \cdot \left(\mathbf{g}_1^T \cdot \hat{\mathbf{r}} \right) \left(\hat{\mathbf{r}}^T \cdot \mathbf{g}_2 \right) \right)$$

If the ZFS is collinear with the Co-Co direction (Fig 1, right), then the preceding formula simplifies to the following

$$D_{dip}^{3/2} = \mu_B^2 \hbar^2 \frac{\mu_0}{4\pi r^3} \left(\mathbf{g}_1^T \cdot \mathbf{g}_2 - 3 \cdot \left(\mathbf{g}_1^T \cdot \hat{\mathbf{r}} \right) \left(\hat{\mathbf{r}}^T \cdot \mathbf{g}_2 \right) \right)$$

$$D_{dip}^{3/2}\left(r_{Co-Co} \parallel z_{ZFS}\right) = \mu_B^2 \hbar^2 \frac{\mu_0}{4\pi r^3} \left(\begin{pmatrix} g_x & & \\ & g_y & \\ & & g_z \end{pmatrix} \begin{pmatrix} g_x & & \\ & g_y & \\ & & g_z \end{pmatrix} - 3 \left(\begin{pmatrix} g_x & & \\ & g_y & \\ & & g_z \end{pmatrix} \cdot \begin{pmatrix} 0 \\ 0 \\ 1 \end{pmatrix} \right) \left((0\,0\,1) \begin{pmatrix} g_x & & \\ & g_y & \\ & & g_z \end{pmatrix} \right) \right)$$

$$D_{dip}^{3/2}\left(r_{Co-Co} \parallel z_{ZFS}\right) = \mu_B^2 \hbar^2 \frac{\mu_0}{4\pi r^3} \left(\begin{pmatrix} g_x^2 & & \\ & g_y^2 & \\ & & g_z^2 \end{pmatrix} - 3 \begin{pmatrix} 0 & & \\ & 0 & \\ & & g_z^2 \end{pmatrix} \right)$$

$$D_{dip}^{3/2}\left(r_{Co-Co} \parallel z_{ZFS}\right) = \mu_B^2 \hbar^2 \frac{\mu_0}{4\pi r^3} \begin{pmatrix} g_x^2 & & \\ & g_y^2 & \\ & & -2g_z^2 \end{pmatrix}$$

For the axial case (E/D = 0), using eq. 12 we then have for the effective dipolar tensor.

$$\begin{aligned} D_{dip}^{1/2}\left(r_{Co-Co} \parallel z_{ZFS}\right) &= \mu_B^2 \hbar^2 \frac{\mu_0}{4\pi r^3} \begin{pmatrix} 4g_x^2 & & \\ & 4g_y^2 & \\ & & -2g_z^2 \end{pmatrix} \\ &= \mu_B^2 \hbar^2 \frac{\mu_0}{4\pi r^3} \begin{pmatrix} g_x'^2 & & \\ & g_y'^2 & \\ & & -2g_z'^2 \end{pmatrix} \end{aligned} \qquad (14)$$

The last step is strictly true when the ZFS is axial.[2] Now in the case that the Co-Co direction is in the *x* direction of the ZFS tensor (or the *y* direction, which is the same for axial ZFS), (Figure S3, left) we get

$$D_{dip}^{3/2}\left(r_{Co-Co}\,\square\, z_{ZFS}\right)=\mu_B^2\hbar^2\frac{\mu_0}{4\pi r^3}\begin{pmatrix}-2g_x^2 & & \\ & g_y^2 & \\ & & g_z^2\end{pmatrix}$$

$$D_{dip}^{3/2}\left(r_{Co-Co}\,\square\, z_{ZFS}\right)=\mu_B^2\hbar^2\frac{\mu_0}{4\pi r^3}\begin{pmatrix}-2g_x^2 & & \\ & g_y^2 & \\ & & g_z^2\end{pmatrix}$$

$$D_{dip}^{1/2}\left(r_{Co-Co}\,\square\, z_{ZFS}\right)=\mu_B^2\hbar^2\frac{\mu_0}{4\pi r^3}\begin{pmatrix}-2\cdot 4g_x^2 & & \\ & 4g_y^2 & \\ & & g_z^2\end{pmatrix}$$

$$=\mu_B^2\hbar^2\frac{\mu_0}{4\pi r^3}\begin{pmatrix}-2\cdot g_x'^2 & & \\ & g_y'^2 & \\ & & g_z'^2\end{pmatrix}$$

The previous relations make it very plausible that in general, for two Co(II) ions, disregarding any similarity or coaxiality

$$D_{dip,eff}^{1/2}=\mu_B^2\hbar^2\frac{\mu_0}{4\pi r^3}\left(\mathbf{g}_1'^T\cdot\mathbf{g}'_2-3\cdot\left(\mathbf{g}_1'^T\cdot\hat{\mathbf{r}}\right)\left(\hat{\mathbf{r}}^T\cdot\mathbf{g}'_2\right)\right)$$

and, assuming for now coaxiality of ZFS tensors,

$$\mathbf{J}_{ani,full}^{1/2}=\begin{pmatrix}J_x^{1/2} & & \\ & J_y^{1/2} & \\ & & J_z^{1/2}\end{pmatrix}$$

$$=\begin{pmatrix}J_x^{3/2}\left(1+\frac{1-3\lambda_A}{\sqrt{1+3\lambda_A^2}}\right)\left(1+\frac{1-3\lambda_B}{\sqrt{1+3\lambda_B^2}}\right) & & \\ & J_y^{3/2}\left(1+\frac{1+3\lambda_A}{\sqrt{1+3\lambda_A^2}}\right)\left(1+\frac{1+3\lambda_B}{\sqrt{1+3\lambda_B^2}}\right) & \\ & & J_z^{3/2}\left(1-\frac{2}{\sqrt{1+3\lambda_A^2}}\right)\left(1-\frac{2}{\sqrt{1+3\lambda_B^2}}\right)\end{pmatrix}$$

where $\lambda_{A,B}$ is the rhombicity parameter of Co(II) A or B. And probably, in general (no more coaxiality)

$$\mathbf{J}^{1/2}_{ani,full} = \mathbf{P}_1^T \cdot \mathbf{J}^{3/2}_{ani,full} \cdot \mathbf{P}_2$$

$$\mathbf{J}^{1/2}_{ani,full} = \mathbf{R}_A \cdot \begin{pmatrix} g'_{xA}/g_{xA} & & \\ & g'_{yA}/g_{yA} & \\ & & g'_{zA}/g_{zA} \end{pmatrix} \cdot \mathbf{R}_A^T \cdot \mathbf{J}^{3/2}_{ani,full} \cdot \mathbf{R}_B \cdot \begin{pmatrix} g'_{xB}/g_{xB} & & \\ & g'_{yB}/g_{yB} & \\ & & g'_{zB}/g_{zB} \end{pmatrix} \cdot \mathbf{R}_B^T$$

where $\mathbf{R}_{A,B}$ are the rotation matrices (eigenvector matrices of the $\mathbf{g}'_{A,B}$ matrices). The coefficients g'_x/g_x are simply the Pilbrow relations. The last formula is probably very complicated to be analytically derived in general, but it can be demonstrated by simulation of the resonances of an arbitrary system considered as real spins and effective spins.

$$\begin{aligned} \hat{H}_{12} &= \hat{H}_{Z,1} + \hat{H}_{Z,2} + \left(\mathbf{P}_1 \cdot \hat{\mathbf{S}}_1^{1/2}\right)^T \cdot \mathbf{D}_{12}^{HS} \cdot \left(\mathbf{P}_2 \cdot \hat{\mathbf{S}}_2^{1/2}\right) \\ &= \hat{H}_{Z,1} + \hat{H}_{Z,2} + \left(\hat{\mathbf{S}}_1^{1/2}\right)^T \cdot \mathbf{P}_1^T \cdot \mathbf{D}_{12}^{HS} \cdot \mathbf{P}_2 \cdot \left(\hat{\mathbf{S}}_2^{1/2}\right) \\ &= \hat{H}_{Z,1} + \hat{H}_{Z,2} + \left(\hat{\mathbf{S}}_1^{1/2}\right)^T \cdot \mathbf{D}_{12}^{1/2} \cdot \left(\hat{\mathbf{S}}_2^{1/2}\right) \end{aligned} \qquad (15)$$

with $\hat{H}_{Z,1(2)}$ given by

$$\begin{aligned} \hat{H}_Z^{1/2} &= \mu_B B^T \cdot \mathbf{g}' \cdot \hat{\mathbf{S}}^{1/2} \\ &= \mu_B B^T \cdot \mathbf{g} \cdot \mathbf{P} \cdot \hat{\mathbf{S}}^{1/2} \end{aligned} \qquad (16)$$

5. Numerical calculations on interacting pairs containing S = 5/2 ions

The previous forms of the expressions for effective interactions between S = 3/2 ions have a form which appears to be general. Therefore, instead of trying to apply the same reasoning to S = 5/2 or higher systems, which provide analytically much more complicated expressions, we will assume the obtained equations are applicable and just verify them numerically. Figure S4 shows two simulations of the energy levels as a function of the

magnetic field, each for a spin pair composed by an S = 5/2 Fe(III) (S´ = 1/2 corresponding to the lower doublet) and an S = 1/2 Cu(II). The black lines are the exact results obtained using S = 5/2 for an Fe(III), while the red lines where obtained assuming an effective S´ = 1/2, with effective *g´*-values and the effective expressions for the interactions.

Simulation parameters are presented in Table S2. In Simulation 1 a high symmetry situation was chosen. For Simulation 2 the **g**-matrices (effective and real) were arbitrarily rotated. This rotation of the **g**-matrices causes a highly anisotropic and antisymmetric effective exchange interaction tensor $\mathbf{J}_{eff}$ between the Fe(III) and Cu(II) spins. In this simulation the maximum value of the real anisotropic exchange interaction $\mathbf{J}_{ani}$ is 45000 MHz = 1.5 cm^{-1}, which is 6.66 times lower than the *D*-value chosen for Fe(III). This is an approximate limit given by the perturbation approach used to derive the relations. If the real $\mathbf{J}_{ani}$ tensor was doubled, small discrepancies between the real spin and effective spin simulations started to show.

Table S2. Simulation parameters for the pair of high spin Co(II) ions corresponding to Figure 1.

Simulation 1

	ZFS	Euler Rotation Angles[a]	Real **g**-matrix	Effective **g´**-matrix
Fe(III)	D = 10 cm^{-1}	α = 0º	g_x = 2.00	2.7406
	E/D = 0.15	β = 0º	g_y = 2.00	8.6623
		γ = 0º	g_z = 2.00	1.4468
Cu(II)	-	α = 0º	g_x = 2.05	Idem
	-	β = 0º	g_y = 2.05	Idem
		γ = 0º	g_z = 2.25	Idem

Real Interaction (MHz)[b]			Effective Interaction (MHz)[b]		
1971.0	0	0	2700.9	0	0
0	1971.0	0	0	8536.9	0
0	0	-4326.7	0	0	-3129.9

Simulation 2

	ZFS	Euler Rotation Angles[a]	Real **g**-matrix	Effective **g´**-matrix
Fe(III)	D = 10 cm^{-1}	α = -30º	g_x = 2.00	2.7406
	E/D = 0.15	β = 150º	g_y = 2.00	8.6623
		γ = 0º	g_z = 2.00	1.4468
Cu(II)	-	α = 20º	g_x = 2.05	Idem
	-	β = 80º	g_y = 2.05	Idem
		γ = 40º	g_z = 2.25	Idem

Real Interaction (MHz)[c]			Effective Interaction (MHz)[c]		
22500	0	0	39683.8	24982.2	-27028.4
0	22500	0	24982.2	80795.8	-28846.9
0	0	45000	-13514.2	-14423.4	48157.9

[a]The **D**-tensors and real **g**-matrices for each Co(II) ion are assumed coincident and the Euler rotation angles are randomly chosen to illustrate the generality of the model.

[b]The simulated interaction is magnetic dipolar, with the Fe(III)-Cu(II) vector chosen in the common frame *z*-direction and an inter ion distance of 3 Å.

[c]Interaction is electronic exchange. The effective interaction tensor is both anisotropic and antisymmetric due to the non-coincidence and anisotropy of the **g** and **g**´-matrices.

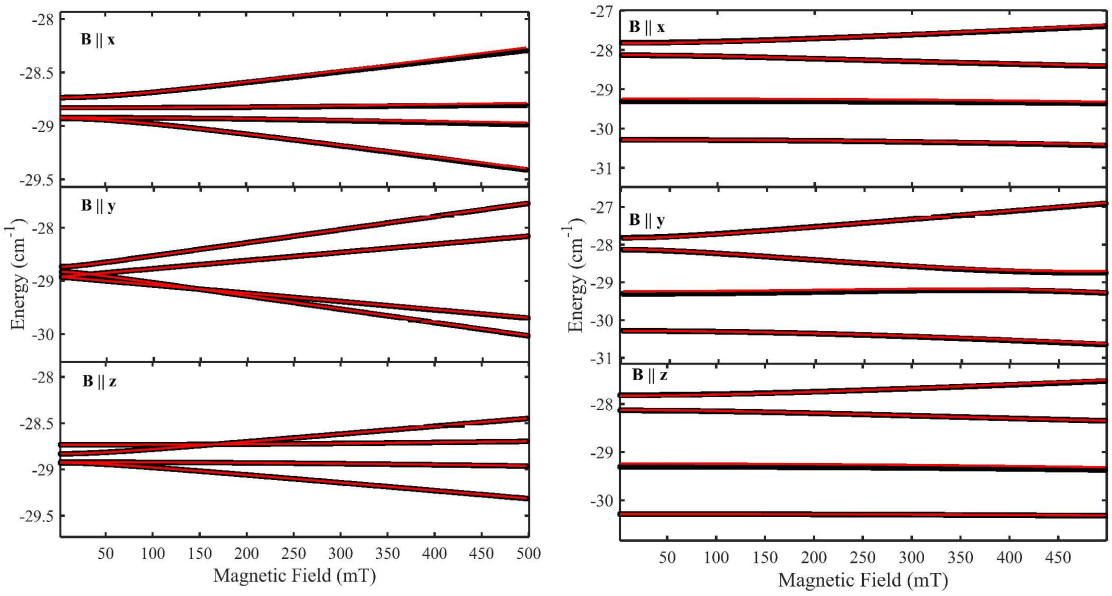

Figure S4. Energy levels of a dimer composed by an S = 5/2 ion and an S = 1/2 ion, with the S = 5/2 ion treated as a real spin (black) and effective S´= 1/2 spin (red). Left: Parameters given in Table S2 (Simulation 1). Right: Parameters given in Table S2 (Simulation 2).

6. Simulation of EPR Spectra of pairs containing high-spin Co(II), Fe(III) or Cu(II) and a nitroxide radical

Figure S5 shows simulations performed with EasySpin[11] of metal-nitroxyl interacting systems with metals of different spin states (Co(II): S = 3/2, $M_S = \pm 1/2$, g'-values = 5.00, 5.00, 2.60; Fe(III): S = 5/2, $M_S = \pm 3/2$, g'-values = 4.3, 4.3, 4.3; Cu(II): S = 1/2, g-values = 2.06, 2.06, 2.25), while nitroxyl is an quasi isotropic S = 1/2 spin (g-values = 2.0088, 2.0061, 2.0027, hyperfine A-values = 15.46, 16.84, 92.5 MHz). The spin-spin distance was 15 Å with the vector parallel to the z-direction.

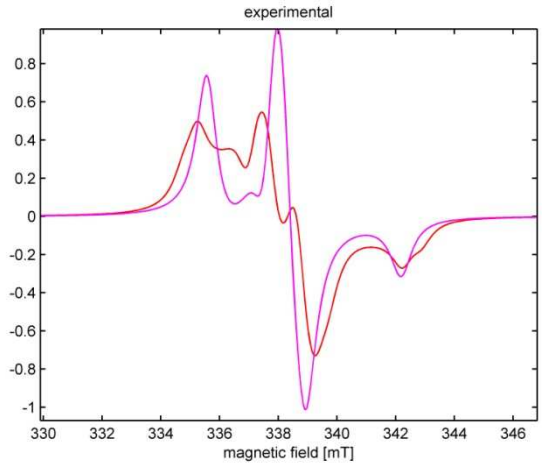

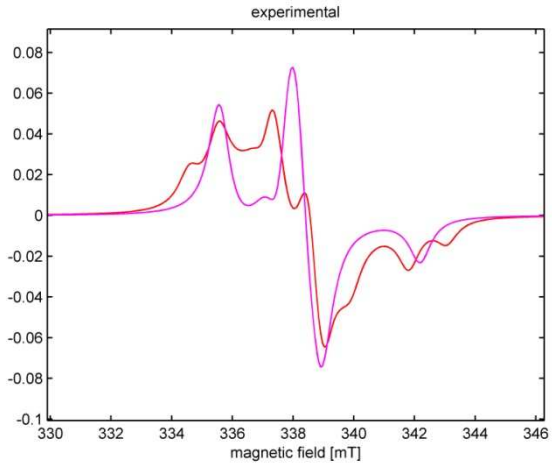

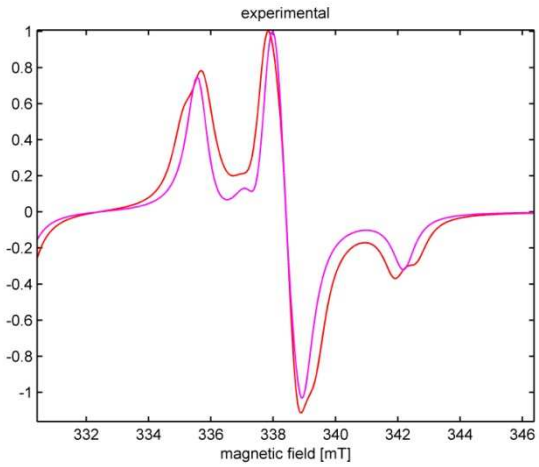

Figure S5. Top: HS Co(II)-NR. Middle: HS Fe(III) (g = 4.3, M_S = ±3/2)-NR. Bottom: Cu(II)-NR. In all cases the spin-spin distance was 15 Å and a purely magnetic dipolar interaction was assumed, using effective g-matrices for HS Co(II) and Fe(III) and real **g**-matrices for Cu(II) and the nitroxide radical. More simulation parameters are indicated in the text.

7. Magnetic Properties of Dysprosium-containing pairs.

Dysprosium(III) ([Xe]4f^9) possesses a ground state multiplet $^6H_{15/2}$ with S = 5/2 and L = 5, giving a total J = 15/2. The real g_J value associated with the J multiplet is given by[4]

$$g_J = 1 + \frac{J(J+1) + S(S+1) - L(L+1)}{2J(J+1)} \qquad (17)$$

and for dysprosium(III) this gives g_J = 1.333. Crystal field operators split the J-multiplet into M_J doublets, and the ground state will depend on the relative magnitudes of the crystal field operator terms.

If only axial crystal field terms are added to the spin Hamiltonian, these ground state doublets will be pure and the effective **g**′-matrix will be $g'_x = g'_y = 0$, $g'_z = g_J(2|M_J|)$. This is exemplified with the spin Hamiltonian

$$\hat{H}_{CF,axial} = B_2^0 O_2^0 + B_4^0 O_4^0 + B_6^0 O_6^0 \qquad (18)$$

with the expressions for the higher order crystal field terms given by Stevens.[12] A simulation of the energy levels of this Hamiltonian plus a Zeeman term in the *x*, *y*, *z* directions is given in Figure S6 and the crystal field parameters are given in the corresponding legend.

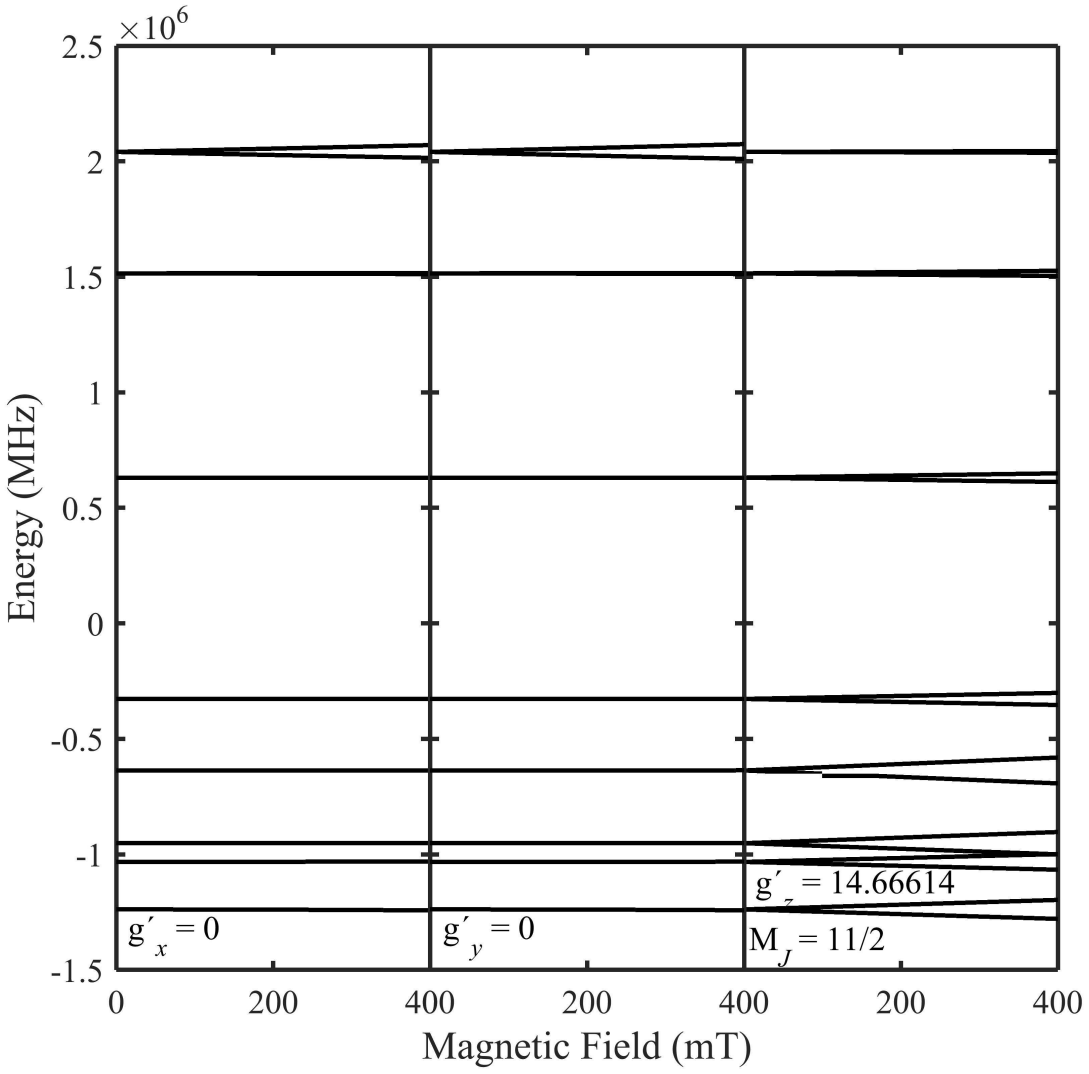

Figure S6. Energy levels of the J = 15/2 multiplet of Dy(III) in the presence of an axial crystal field, given by eq. (18), with crystal field parameters B_2^0 = -80 cm^{-1}, B_4^0 = -40.8 cm^{-1} and B_6^0 = -8 cm^{-1}, B_2^2 = -0.02 cm^{-1}, with the magnetic field pointing in the directions given by the effective g'-values. The low crystal field values were chosen to qualitatively show all the energy levels and their Zeeman splitting in the magnetic field; however in real compounds these will be much larger (see chapter 5 in ref. [4]).

Compounds with negative and strictly axial crystal field operators will give $M_J = \pm 15/2$, $\pm 13/2$ or $\pm 11/2$ ground states, with $g'_x = g'_y = 0$, and therefore will be EPR-silent, although their ability to magnetically interact with other spins will not be impaired, as shown in the work of Pineda *et al.*[13]

Application of the effective magnetic interaction model to Dy(III) dimers present a complication compared with dimers containing HS Co(II) or Fe(III), because effective **g**′-matrix formulas for Dy(III) ions in arbitrary crystal fields do not exist. These perhaps could be derived under some situations, but this would exceed the purpose of this work. Instead our approach has been to develop a program (*Jmultiplet_zfs*) which simulates the energy levels of a Dy(III) ion under the action of a crystal field Hamiltonian containing O_2^0, O_4^0, O_6^0 and O_2^2 terms, together with Zeeman interaction. Many other crystal field terms could be easily added (see Table 16 in Abragam and Bleaney's book[4]). The program plots the energy levels for the magnetic field in the *x*, *y* and *z* directions, and calculates the effective *g*′-values. The user can change crystal field parameters, the total *J* of the ion (thus allowing simulation of other lanthanides), the L and S values, which allow calculation of g_J using eq. (17), and some other quantities.

With the calculated effective *g*′-values for a certain ion obtained using *Jmultiplet_zfs* and the definition of a real magnetic interaction matrix, another program, called *Ln_Dimer_Levels*, simulates the energy levels of a dimer as a function of magnetic field.

A simulation of a weakly coupled Dy(III) dimer is shown in Figure S7. The red lines are simulations using effective interactions for effective $J' = 1/2$ Dy(III) sites, while the black dots use the full $J = 15/2$ space for each center, together with crystal field parameters. The non-typical shape of the dimer levels (absence of clear singlet and a triplet groups) is due to

the very high deviation from null-trace in the effective Dy(III)-Dy(III) interaction tensor, caused by the high anisotropy of the effective **g**′-matrices. The agreement in the *z*-direction is excellent, and this is the most important magnetic direction for Dy(III) (with $g'_z \sim 13\text{-}20$). The agreement in the other two directions is not perfect, but it is quite good, as the separation between the two doublets is correctly reproduced, but the exact curvature of the levels on each doublet is not perfectly reproduced. The agreement between the real and effective spin models starts to break down when the real exchange has such a value that the splitting between the lowest two Kramers' pairs becomes equal with the splitting between the first and third Kramers' pairs. We will not attempt to derive explicit bounds for the J_{AB}^{real}/Crystal Field terms as there will be many different possibilities. However, as the *Ln_Dimer_Levels* program shows all real spin energy levels, any interested users can experiment themselves to test the validity of the model as it applies to their specific systems. For this system, J_{AB}^{real} up to 30000 MHz gives a good agreement. This can be seen in Figure S8.

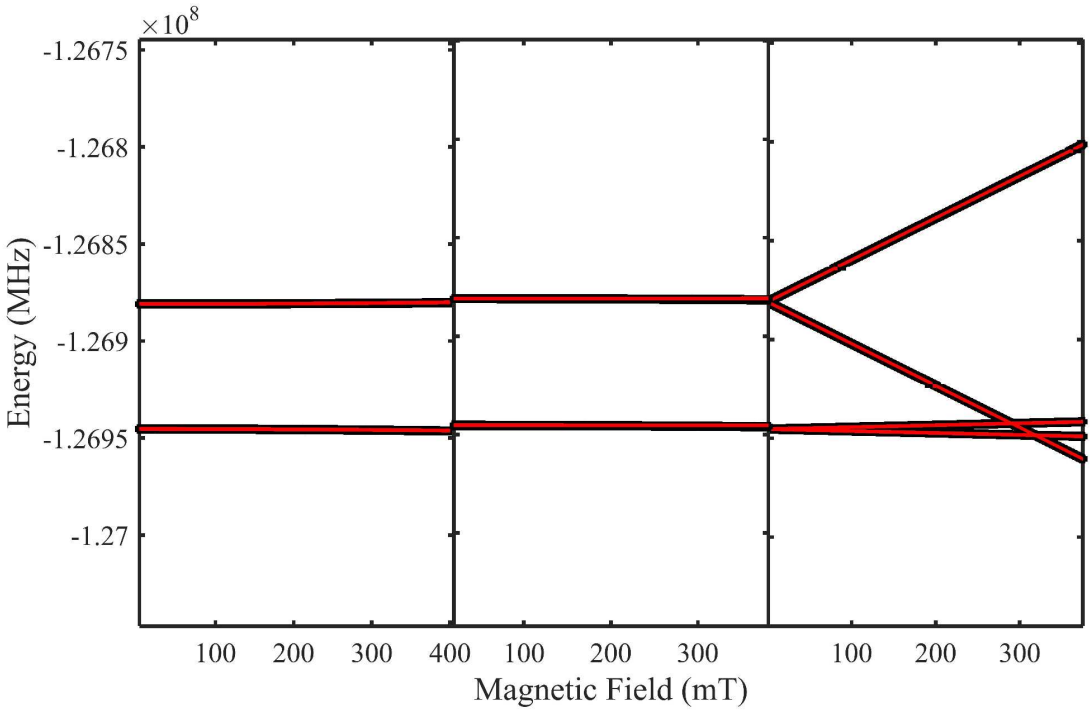

Figure S7. Energy levels for a hypothetical Dy(III) dimer with the magnetic field pointing in the *x* (left), *y* (right) and *z* (direction) of both Dy(III) ions. The black dots show the energy levels using the full $J = 15/2$ space for each ion (total 256 by 256 matrix) and the following Hamiltonian parameters (Dy_A: $B_2^0 = 3200$ cm^{-1}, $B_4^0 = -1440$ cm^{-1}, $B_6^0 = -400$ cm^{-1}, $B_2^2 = 22$ cm^{-1}, $g_J = 1.33333$; Dy_B: $B_2^0 = 4000$ cm^{-1}, $B_4^0 = -1040$ cm^{-1}, $B_6^0 = -400$ cm^{-1}, $B_2^2 = -50$ cm^{-1}, $g_J = 1.33333$; $J_{AB,iso}^{real} = 1000$ MHz (0.0333 cm^{-1})), while the red lines show the energy levels of the effective $J' = 1/2$ subspace (total 4 by 4 matrix), with the following parameters (Dy_A: $g'_x = 0.103295$, $g'_y = 0.58509$, $g'_z = 14.44965$; Dy_B: $g'_x = 2.626123$, $g'_y = 0.51238$, $g'_z = 15.84771$; $J_{AB,x}^{eff} = 152.59$ MHz, $J_{AB,y}^{eff} = 168.63$ MHz, $J_{AB,z}^{eff} = 128810$ MHz).

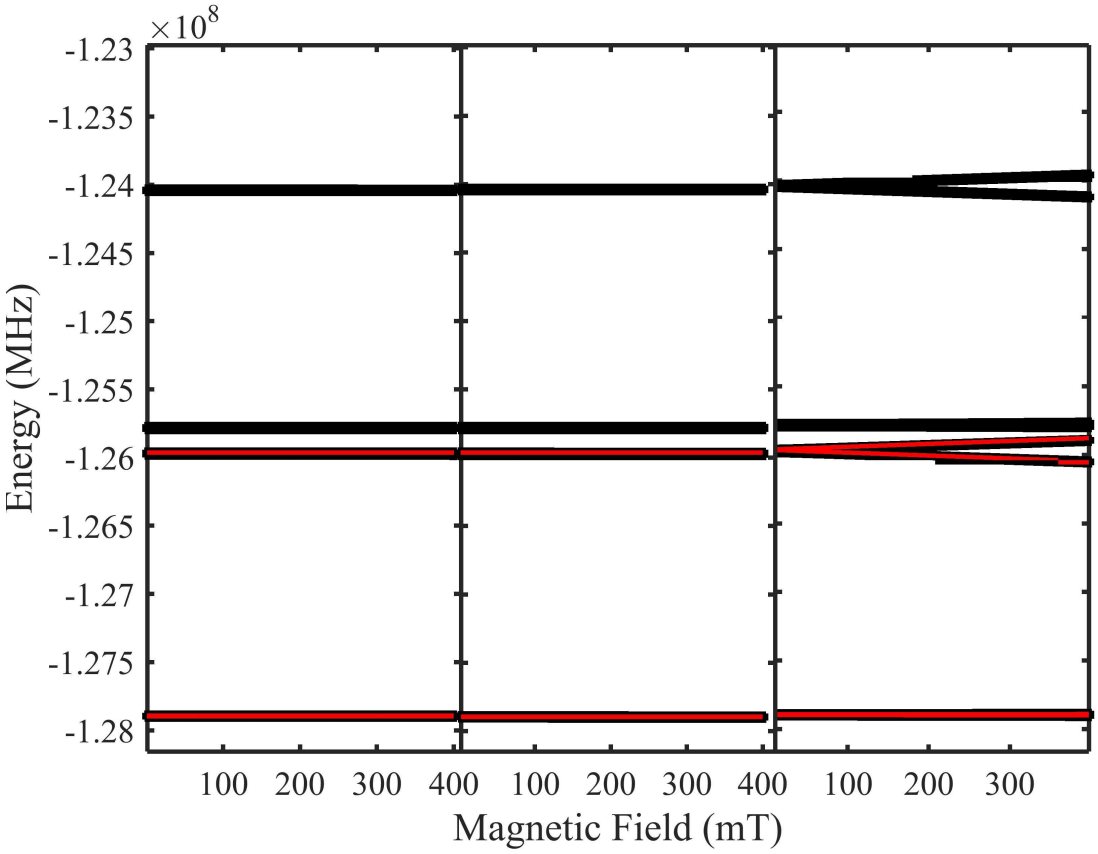

Figure S8. Simulation of the same system as Figure S7, but with $J^{real}_{AB,iso}$ = 30000 MHz (1 cm^{-1})

8. References

1. Kahn, O. *Molecular Magnetism*. VCH Publishers: New York, 1993.
2. Pilbrow, J. R. Effective g values for S = 3/2 and S = 5/2. *Journal of Magnetic Resonance (1969)* **1978,** *31*, 479-490.
3. Pilbrow, J. R. *Transition Ion Electron Paramagnetic Resonance*. Clarendon Press: Oxford, 1990.
4. Abragam, A.; Bleaney, B. *Electron Paramagnetic Resonance of Transition Ions*. Clarendon Press: Oxford, 1970.
5. Rechkemmer, Y.; Breitgoff, F. D.; Van Der Meer, M.; Atanasov, M.; Hakl, M.; Orlita, M.; Neugebauer, P.; Neese, F.; Sarkar, B.; Van Slageren, J. A Four-Coordinate Cobalt (II) Single-Ion Magnet with Coercivity and a Very High Energy Barrier. *Nature communications* **2016,** *7*.
6. Titiš, J.; Boča, R. Magnetostructural D Correlations in Hexacoordinated Cobalt(II) Complexes. *Inorg. Chem.* **2011,** *50*, 11838-11845.

7. Krzystek, J.; Zvyagin, S. A.; Ozarowski, A.; Fiedler, A. T.; Brunold, T. C.; Telser, J. Definitive Spectroscopic Determination of Zero-Field Splitting in High-Spin Cobalt(II). *J. Am. Chem. Soc.* **2004,** *126*, 2148-2155.
8. Suturina, E. A.; Maganas, D.; Bill, E.; Atanasov, M.; Neese, F. Magneto-Structural Correlations in a Series of Pseudotetrahedral [CoII(XR)4]2− Single Molecule Magnets: An ab Initio Ligand Field Study. *Inorg. Chem.* **2015,** *54*, 9948-9961.
9. Schweinfurth, D.; Sommer, M. G.; Atanasov, M.; Demeshko, S.; Hohloch, S.; Meyer, F.; Neese, F.; Sarkar, B. The Ligand Field of the Azido Ligand: Insights into Bonding Parameters and Magnetic Anisotropy in a Co(II)–Azido Complex. *J. Am. Chem. Soc.* **2015,** *137*, 1993-2005.
10. Neuman, N. I.; Winkler, E.; Peña, O.; Passeggi, M. C.; Rizzi, A. C.; Brondino, C. D. Magnetic Properties of Weakly Exchange-Coupled High Spin Co (II) Ions in Pseudooctahedral Coordination Evaluated by Single Crystal X-Band EPR Spectroscopy and Magnetic Measurements. *Inorg. Chem.* **2014,** *53*, 2535-2544.
11. Stoll, S.; Schweiger, A. EasySpin, a Comprehensive Software Package for Spectral Simulation and Analysis in EPR. *J. Magn. Reson.* **2006,** *178*, 42-55.
12. Stevens, K. Matrix elements and operator equivalents connected with the magnetic properties of rare earth ions. *Proceedings of the Physical Society. Section A* **1952,** 65, 209.
13. Pineda, E. M.; Chilton, N. F.; Marx, R.; Dörfel, M.; Sells, D. O.; Neugebauer, P.; Jiang, S.-D.; Collison, D.; van Slageren, J.; McInnes, E. J. Direct Measurement of Dysprosium (III)···Dysprosium (III) Interactions in a Single-Molecule Magnet. *Nature communications* **2014,** *5*.